RSC Advances

PAPER

View Article Online
View Journal | View Issue

Cite this: *RSC Adv.*, 2017, **7**, 22145

Manipulating selective dispersion of reduced graphene oxide in polycarbonate/nylon 66 based blend nanocomposites for improved thermo-mechanical properties†

Santosh Kr. Tiwari,[a] Kartikey Verma,[b] Pupulata Saren,[a] Ramesh Oraon,[a] Amrita De Adhikari,[a] Ganesh Chandran Nayak*[a] and Vijay Kumar*[b]

Received 18th February 2017
Accepted 10th April 2017

DOI: 10.1039/c7ra02044a

rsc.li/rsc-advances

This work explored the thermo-mechanical properties of a reduced graphene oxide (rGO) based polycarbonate/nylon 66 blend system. Synthesis of rGO is carried out *via* a facile solid-state reduction of GO, using selenium powder. Selective dispersion of rGO was achieved by varying the mixing-sequence of rGO in the polymer matrices under controlled shear pressure. Selective dispersion of rGO in the blend system has been investigated with FTIR, FESEM and a rheometer. FTIR analysis showed the preferential localization of rGO in the nylon phase when it melt blended first with nylon followed by PC. In addition, the mechanical and thermal properties of this blended system were also found to be higher than those of other blend nanocomposites. The rheological study showed that lower viscosity of nylon could be the reason for preferring dispersion of rGO in the nylon phase when blended first with nylon. This preferential localization of rGO in the nylon phase affects the crystallization of the nylon phase and interfacial adhesion which resulted in enhanced mechanical strength and chemical inertness of the blend nanocomposite.

1. Introduction

The present era of materials science has found polymers to be the front-runner for many applications in the field of science and technology. Among various applications, heavy industries require a polymeric material with high mechanical strength, consistency under drastic conditions, and versatility in different working atmospheres with reliable electrical and thermal properties.[1,2] However, it is very difficult to find or synthesize a single polymer which possesses all of these properties. To achieve the targeted properties, different polymers, having unique properties, are blended together in different proportions to produce a product with properties better than those of the individual polymers.[3,4] In addition, the properties of polymer blends can be tailored by coalescing blend partners and this can be used to recycle polymers for various applications.[3–6] However, most of the polymers are incompatible in nature which can deteriorate the properties of polymer blends as compared to their individual constituents. Hence, it is very crucial to reduce phase separation and enhance interfacial adhesion between blend components for the anticipated properties.[7,8] The most convenient and economical path to achieve a single glass transition temperature (*i.e.* negligible phase separation) is by incorporation of suitable fillers into polymers that will extend the potential use of the resulting materials.[9,10] In this line, many research groups were dedicated their study to explore impact of different fillers on properties polymer blends[11] and in the recent years polymer scientist have studied a series of micro and nanofiller like grafted compatibilizer,[12] copolymers,[13] carbon black,[14] graphite,[15] fiber,[16] glass fiber,[17] fly ash,[18] nano clay,[19] nanosilica,[20] carbon nanotubes (CNTs),[21,22] and graphite derivatives.[15,23,24] And they have explored their influence on the internal morphology, compatibility, miscibility, conductivity and mechanical properties of blended materials.[12,25] In the present work to insert some specific properties, we have focused on nylon 66/polycarbonate based polymer blends. Nylon 66 and polycarbonate are well-known for wide range industrial applications.[26] These two polymers are considered to be the backbone of electrical industries, automobile industries and toy industries and a million tons of nylon 66/polycarbonate manufactured annually.[26] Nylon 66 is moisture absorbing, shows significant shrinkage in molded part, and attacked by strong oxidizing chemicals,[26] on other hand polycarbonate is comparably expensive, marring, notch sensitivity, greatly sensitive to abrasive cleaners and wracked by some alkaline cleaning products.[27] To avoid these lacunae we have

[a]*Department of Applied Chemistry, Indian Institute of Technology (ISM), Dhanbad, Jharkhand, India. E-mail: nayak.g.ac@ismdhanbad.ac.in; Tel: +91 326-2235934*

[b]*Department of Applied Physics, Chandigarh University, Gharuan, Mohali, Punjab, India. E-mail: vj.physics@gmail.com*

† Electronic supplementary information (ESI) available. See DOI: 10.1039/c7ra02044a

used rGO as nanofiller for nylon 66/polycarbonate blend. The rGO is predominantly sp^2 hybridized few atoms-thick 2D carbon layers with some oxygen containing functional groups at the edges, has been treated as front line nanofiller due to its enthralling physical and chemical properties such as extraordinary electrical, mechanical, and thermal properties.[28,29] It has widely been studied in the various fields of science and technology.[28–30]

The fabricated nylon 66/polycarbonate blend is of greater importance because of the suitable interaction between the rGO nano sheets and polymer chains (bonding interaction between –OH, –COOH of rGO and –NH of nylon 66 and oxygen functional groups of PC along with this there is a great probability for hydrogen bonding among the functional moieties of polymer chains and rGO nano sheets[32,33]). These interactions significantly minimize phase separation between the blend partners.[31,32] These interactions take place in such a controlled way that possibilities for aggregation of rGO become very insignificant.[33] To explore selective dispersion of rGO nanosheets we have used the concept of mixing sequence during the processing of polymer blend nanocomposites (PNCs). The mixing sequence makes very easy to identify migration of rGO nano sheets into an individual blend partner. Herein, for the melt compounding, we have used controlled shear processing twin screw extruder. This processing technique greatly enhances homogeneous dispersion of rGO into nylon 66 and polycarbonate.[34] Moreover, the chemical inertness of the developed blends has been tested in the different solvents and it has been found that mixing sequence played a crucial role to define solubility of the fabricated blend systems.[34,35] To the best of our knowledge, we are reporting the first-time use of rGO nano sheets as nanofiller for nylon 66/polycarbonate in the light of mixing sequence and its effect on thermo-mechanical properties, chemical resistance and microstructures of blend nanocomposites.

2. Experimental

2.1 Materials

All the chemical reagents used for synthesis, reduction and purification of rGO such as graphite powder, potassium permanganate ($KMnO_4$), sulfuric acid (H_2SO_4, 98%), orthophosphoric acid (H_3PO_4, 88%), hydrogen peroxide (H_2O_2, 30%), selenium powder (particle size: 100 mesh), and hydrochloric acid (HCl, 10%), were procured from Sigma Aldrich (India) with purity levels of >99.9%. However, nylon 66 (PXR-01NC, Next polymers Pvt. Ltd. Mumbai)/polycarbonate (Makrolon® 2405), Bayer materials science (Thailand) used in the present investigation were procured from JP Polymers and Gkhanna Co. Mumbai, respectively. Polycarbonate is an aromatic copolymer while nylon 66 is a completely aliphatic polymer.

2.2 Synthesis of graphene oxide

For the synthesis of graphene oxide (GO) we have adopted a procedure developed by Marcano *et al.*[36] In brief, graphite powder (6.0 g, 1 wt equiv.) were oxidized using a mixture of concentrated H_2SO_4/H_3PO_4 in 9 : 1 ratio (720 : 80 mL) along with the very slow addition of $KMnO_4$ powder (36 g, 6 wt equiv.). The addition of $KMnO_4$ is a slight exothermic (around 40 °C) step. After the completion of KMnO4 addition, the reaction mixture was heated up to 60 °C and stirred continuously for 15 h. Then reaction mixture was cooled to room temperature and transferred to an ice bath (500 mL) with drop-wise slow addition of 30% H_2O_2 (6 mL) in a dark chamber. For work-up, the reaction mixture was neutralized (pH around 6.5 slightly acidic) by multiple washing with the distilled water and then centrifuged@3000 rpm for 2 h, and then supernatant materials was decanted away. Now the residual material was washed in a sequence with 400 mL of distilled water, 400 mL of 30% HCl, and 400 mL of ethanol. Finally, the solution was filtered over a PTFE membrane. The product obtained on the PTFE membrane (graphene oxide nearly 10 g) was dried in a vacuum for 48 h at 45 °C.

2.3 Conversion of GO to rGO using selenium powder as a reducing agent

For the bulk amount rGO, we have adopted a time efficient reduction strategy recently developed by our own research group using Se powder.[37] The reduction methodology briefly mentioned as; 0.3 g of ultrapure Se powder was used for the reduction of 3 g fully exfoliated GO nano sheets to rGO. Moisture free GO and Se powder were mixed well using mortar and pestle and then the mixture is sealed in a quartz tube, under an inert atmosphere. The tube was placed in a furnace at 360 °C for 5 minutes. The resulted product was washed thoroughly with distilled water to eliminate impurities.[37]

2.4 Preparation of nylon 66/polycarbonate/rGO blend nanocomposites

Prior to compounding, nylon 66, polycarbonate and rGO were well dried at 80 °C under air oven for 10 h. The neat blend and the rGO filled nanocomposites were synthesized through melt

Table 1 Code and composition of studied polymeric materials

S. no.	Sample code	Composition and mixing order	Processing conditions
1	P	Polycarbonates (100%)	Temp 270 °C, RPM = 10
2	N	Nylon 66 (100%)	Same
3	P/N66	Nylon 66 (70%) + polycarbonates (30%)	Same
4	PNG	Polycarbonates (29.5%) + nylon 66 (69.5%) + reduced graphene oxide (1%)	Same
5	PGN	Polycarbonates (29.5%) + reduced graphene oxide (1%) + nylon 66 (69.5%)	Same
6	NGP	Nylon 66 (69.5%) + reduced graphene oxide (1%) + polycarbonates (29.5%)	Same

compounding in a twin-screw extruder (Fly Tech Engineering, Chennai, India) with shear rotation 10 rpm and at 270 °C temperature for 10 min. The diameter of each screw is 20 mm while length/diameter ratio is 15. To assess the effect mixing sequence of rGO on the physical properties of the ternary blends composites, we prepared total three blend nanocomposites on the basis mixing sequence of the rGO. The actual composition of neat blend and polymer blend nanocomposites (PNCs) is summarized in the Table 1. For the testing of mechanical properties we have fabricated six strips of the studied materials using a compression molding machine according to ASTM standard for plastic materials and so prepared strips were cooled at room temperature.

3. Sample characterization

3.1 Characterization of prepared rGO

The details about different characterization techniques (FTIR, UV-Visible, XRD, Raman spectroscopy, XPS analysis, BET surface area, FESEM and TEM micrographs) used for the prepared rGO has been described in our previous work.[28]

3.2 Characterization of prepared PNCs

3.2.1 ATR (attenuated total internal reflectance) – FTIR spectroscopy. FTIR spectra in ATR mode were documented by a Cary 630 FTIR Spectrometer (Agilent Technologies) contacting Diamond ATR contact crystal. All spectra of prepared PNCs were recorded through one time internal reflection at room temperature with a resolution of 4 cm^{-1} and at 32 scans.

3.2.2 XRD patterns. Wide angle X-ray diffraction (WAXD) patterns of as prepared PNCs were analyzed by using a Bruker DS Focus with incident X-ray source Cu Kα ($\lambda = 1.54$ Å) and scan rate 1° per minute from $2\theta = 5$–60°.

3.2.3 DSC analysis. Differential scanning calorimetric analysis of as synthesized PNCs were performed in nitrogen gas environment with a DSC instrument (Model: NETZCH DSC 200 PC instrument). Standardizations of heat flow and temperature were based on a run in which pure indium was heated through its melting point. All the PNCs having a mass of about 20 mg were used for the study up to 300 °C with the heating@10 °C min^{-1} and then cooled at same rate.

3.2.4 TG analysis. TG measurements for as synthesized PNCs were performed under a continuous nitrogen gas purge in a TGA instrument (DuPont TGA-2100 thermal analyzer). All the PNCs having a mass of about 30 mg were used for the analysis from RT to 450 °C with a heating@10 °C min^{-1}.

3.2.5 Scratch hardness and depth indentation analysis. We have used 270VRSD Hardness Tester instrument to investigate scratch hardness and depth indentation of prepared PNCs. This instrument is fully automatic control and commands can be preloaded through software (AFFRI® patent). Pushing the Start button, of instrument its head moves down to reach the test surface from distance multiples of 50 mm and automatically starts the hardness test cycle in automatic succession without breaching a phase. The indentation experiment was carried out at the room temperature and at a relative humidity of 40%. The indentation tests using a Berkovich indenter head (equivalent cone angle 70.3° shown in the Fig. 5).

3.2.6 Mechanical properties testing. Young's modulus, elongation, and tensile test of synthesized PNCs were carried out on a dumb-bell shaped samples using UTM instrument (model no. Hounsfield HS 10 KS) operated at room temperature with a gauge length of 30 mm and with a load cell of 10 kilo newton at a crosshead speed@1 mm min^{-1}.

3.2.7 FESEM analysis. The surface morphology and fractured surfaces of the prepared blends were analyzed FESEM instrument (model no. Supra 55 Carl Zeiss, Germany) by breaking the samples in liquid nitrogen and then coated by platinum to make samples conducting under an accelerating voltage of 5–7 kV.

4. Results and discussion

4.1 ATR-FTIR spectroscopy

Miscibility of nylon 66 and polycarbonate during melt blending has been reported differently by various research groups. Some

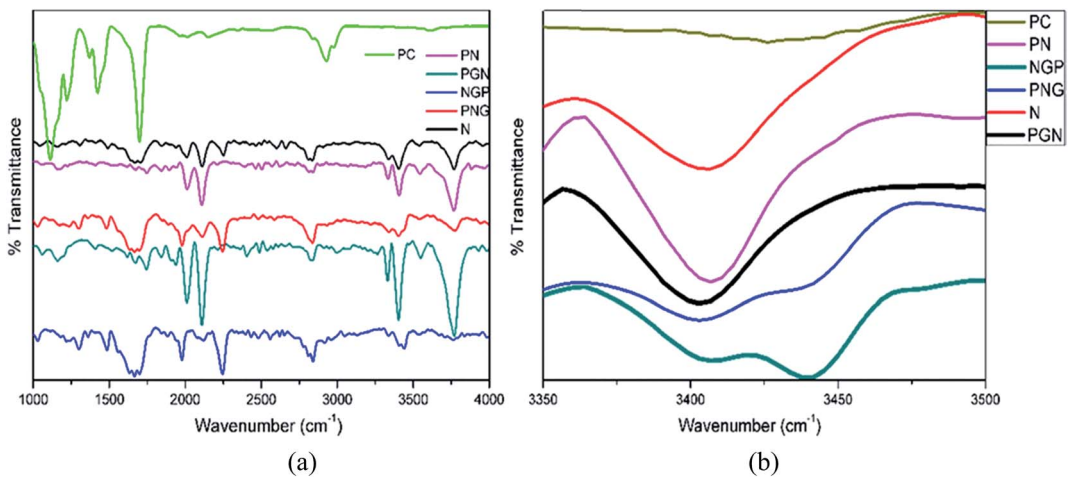

Fig. 1 ATR-FTIR spectra of pure polymers and prepared PNCs (a) full spectra and (b) magnified section.

research groups showed partially miscible nature of the binary blend attributed to the weak non-covalent bonding between the blend partners (when polycarbonate is lower than 40 wt%) on other hand few workers reported that nylon 66/polycarbonate blends are completely immiscible in an asymmetric proportion.[38,39] We have used ATR-FTIR spectroscopy to identify various interactions between blend components and the effect of rGO incorporation on polymer blend nanocmposites.[40] The ATR-FTIR spectra of binary blend and its nanocomposite are shown in Fig. 1. Pure nylon 66 and polycarbonate shows their characteristic IR peaks, including stretching and weak wagging, rocking and bending vibrations.[41,42] To examine interaction between nylon 66 and PC, the N–H stretching frequency of nylon (around 3400 cm^{-1}) has been analyzed, because of a probable interaction between nylon 66 and polycarbonate through (–O···N–H) hydrogen bonding.[32,33] Nylon 66 shows a broad peak at 3404 cm^{-1} corresponding to the N–H stretching, which also observed in the case of binary blend without any change.[32,33] This indicates that there is no interaction between PC and nylon phases. However, incorporation of rGO in nylon/PC blend shows a shoulder peak at 3440 cm^{-1}, in addition to the 3404 cm^{-1} peak. In the absence of any interaction between nylon and PC, this new peak can be ascribed to the interaction of nylon with rGO. Moreover, new peak around 1483 cm^{-1}, attributed to C=C stretching of the rGO, indicates the presence of rGO in blend system.[36,37] Similarly, it can also be observed for the NGP blend system, where rGO was dispersed in nylon matrix, then with a PC, an intense peak at 3440 cm^{-1} is observed. This indicates that while mixing of rGO with nylon phase than with a PC, the rGO sheets remained in the nylon phase without migrating to the PC phase due to which the peak intensity increased at 3440 cm^{-1}. However, in case of a PGN blend system, where rGO was first mix with PC and then with nylon, no peak was observed at 3440 cm^{-1}. This indicates that when rGO was mixed first with PC and then with nylon, the rGO sheets remained in PC phase, without migrating to the nylon phase resulted in no interaction between nylon and rGO and hence the disappearance of 3440 cm^{-1} peak. The presence of very low intensity shoulder peak at 3440 cm^{-1} in PNG blend system can be attributed to partial dispersion of rGO in both nylon and PC phases. To further investigate dispersion behavior of rGO in nylon and PC phases correspond to the change in mixing sequence, XRD analysis was carried out and presented in the following section.

4.2 XRD pattern analysis

XRD patterns of the pure polymers, neat blend and PNCs were recorded at room temperature and presented in the Fig. 2. Pure polycarbonate shows a broad peak around $2\theta = 17°$ showing the amorphous nature of PC and chain separation.[43] Nylon 66 shows two intense diffraction peaks around $2\theta = 20.20°$ and $2\theta = 24.04°$ corresponding to $\alpha 1$ and $\alpha 2$ peaks, which shows the crystalline packing due to inter polymer hydrogen bonding.[44] However, in binary blend (PN), the characteristic peaks of PC and nylon merge together and can be observed as a broad peak, corresponding to PC along with a less intense sharp peak

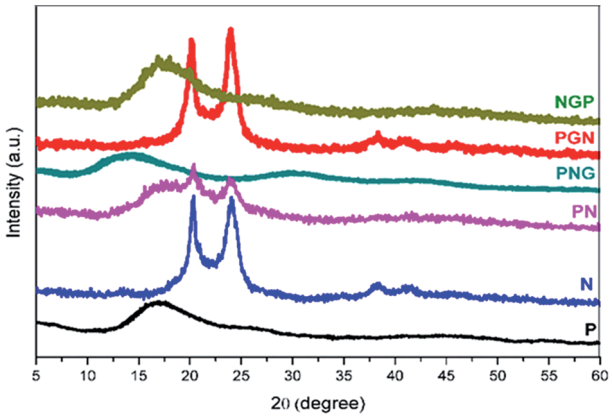

Fig. 2 X-rays diffraction pattern of pure polymers, neat blend and prepared PNCs.

corresponding to nylon 66.[43–45] The broadness of the peak indicates the amorphous nature of the blend. Absence of molecular interaction between PC and nylon is the case of neat blend (as discussed in FTIR section), decreased crystallinity of the blend attributed to penetration of PC chains into a nylon matrix which can disturb the hydrogen bonding interaction within the nylon chains and hence diminished mechanical properties which has also reported in literature.[43,44] However, with the incorporation of rGO in binary blend system, the crystalline peak disappeared, which is an indication of further decrease in molecular interaction between nylon chains. This could be due to the distribution of rGO in the blend matrix and preferably in nylon phase. This also supported by FTIR analysis where N–H peak of nylon changed after the incorporation of rGO. Distribution of rGO in nylon phase can disrupt the hydrogen bonding interaction among nylon chains by acting as a barrier between two chains. Dispersion of rGO in nylon phase could be due to lower viscosity of nylon as compared to PC. The influence of melt viscosity will be discussed in rheology section. Further, the change in mixing sequence of rGO in a blend system completely altered the crystal structure of polymer blends. For instance, PGN blend shows a crystalline structure, NGP shows a complete amorphous nature similar to PNG blend. This can be explained based on the selective dispersion of rGO in PC/nylon blend system.[46] When rGO added to the nylon phase first and then to the PC (NGP) phase, the rGO sheets remained stayed in the nylon phase due to lower viscosity of nylon and hence similar to the PNG system it also acquired an amorphous nature. Interestingly, when rGO mixed with PC phase, it remains persist in PC phase without further migration toward nylon phase and consequently an inter chain interaction in nylon phase was not disturbed and hence crystalline peak corresponding to nylon appeared in the NGP blend system. Also broad peak due to polycarbonate disappeared in NGP blend. This indicates that the dispersion of rGO can be controlled in the PC/nylon blend by varying the mixing sequence. The effect of this dispersion on thermal properties of blend systems were studied by DSC and TGA, respectively and presented in the next section.

4.3 Differential scanning calorimetry (DSC) analysis

Differential scanning calorimetry has been extensively applied in the investigation of various phenomena occurring during the thermal heating of polymeric materials, involving crystallization, glass transition (T_g), curing and melting.[47–49] In order to check above mentioned properties of the synthesized neat blend and three different PNCs, DSC analysis was carried out at a heating rate of 10 °C min^{-1}. Fig. 3 shows the DSC cooling plot of different composites. The peaks corresponds to crystallization of nylon 66 and polycarbonate during the cooling cycle is well defined in the Fig. 3. It is reported that the extent of crystallization of polymeric materials is greatly affected by the incorporation of nanofiller which can act as a nucleating agent.[22,23] In the present study it was observed that with the incorporation of rGO in PNG system, crystallization peaks shifts to a litter higher temperature, which can be attributed to the presence of rGO in nylon phase. However, in XRD analysis we could not able to get any crystallization peak of nylon which may be due to uncontrolled cooling of blends during blending. However, under the cooling cycle of DSC controlled cooling rate exerted proper crystallization. It has also been observed that the area under the curve of PNG system is lesser than the PN system which can be attributed to the crystal growth.[49,50] It supports the XRD analysis where no crystallization was observed. It is believed that the presence of rGO facilitates nucleation but crystal growth got retarded due to the presence of rGO sheets between the nylon chains. For the PNG system, the crystallization temperature matches with that of PN but the area under the curve have reduced significantly.[49–51] This shows that crystallization is not affected by the sequential addition of rGO in PC but does occur with nylon. The reduced peak area indicates that growth has retarded. This can be explained by migration of the small amount of rGO to the nylon phase during blending which does not affect the crystallization temperature but affect to crystal growth. In contrast to this, incorporation of rGO to nylon phase first than to PC phase shows a higher crystallization temperature indicating rapid nucleation but reduced area suggests retarded crystal growth. This analysis shows that the crystallization can be affected by sequential addition of rGO to PC and nylon phase.[22,23] To verify the results of DSC analysis and to evaluate the degradation of neat blend and PNCs thermogravimetric analysis (TGA) was carried out and the graph is presented in Fig. 4.

4.4 Thermogravimetric analysis (TGA)

Thermogravimetric analysis (TGA) is an important technique to probe the thermal stability of pure polymers and their composites.[47] With the suitable experimental conditions, information about the degradation, melting temperature and weight loss corresponding to a particular temperature can be obtained. A typical TGA graph of specimen is shown in Fig. 4. Table 2 is showing the percentage of weight loss corresponding to 1st onset of each sample. It has been observed that the thermal stabilities of the nanocomposites increased as compared to pure blend. Pure blend and all three nanocomposites show less than 5% decomposition in the temperature range up to 300 °C which shows its higher thermal stability as compared to reported works.[52]

From TGA data, it is clear that the incorporation of rGO nanosheets leads to a noteworthy increase in thermal stability for neat blend and PNCs at the initial stage of degradation. This enhancement in the resistance to thermal degradation can be

Table 2 1st onset degradation temperature and corresponding weight loss

Samples	1st onset degradation	% of weight loss corresponding to 1st onset
PN	305.6 °C	3.6
PNG	328.03 °C	4.0
PGN	322.16 °C	7.5
NGP	330.5 °C	0.09

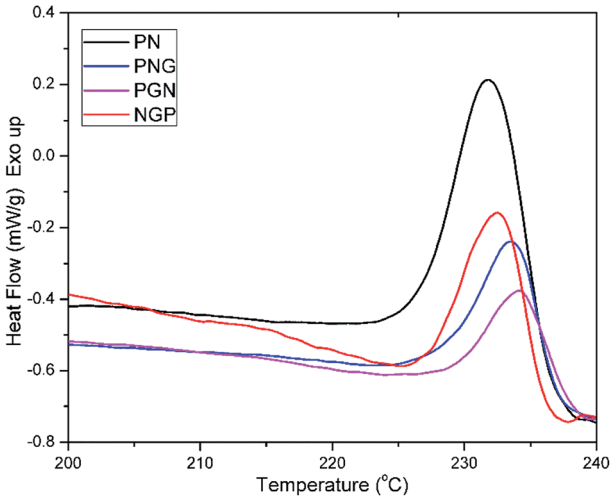

Fig. 3 DSC crystallization temperature of prepared neat blend and PNCs.

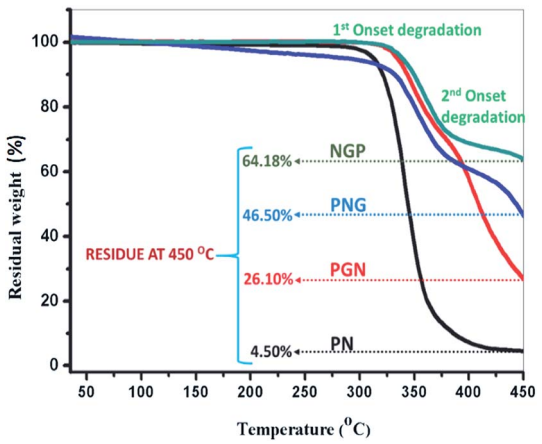

Fig. 4 TGA plot showing 1st and 2nd onset degradation and corresponding weight loss of prepared neat blend and PNCs.

attributed to the hindered diffusion of volatile decomposition products within the PNCs and also owing to selective distribution of rGO through the mixing sequence in polymer blends which favors cross-linking (shown in Fig. 5) between rGO nanosheets–polymer chains.[52,53] This nano-sizing effect is owing to the assimilation of rGO and its selective distribution (as mentioned in DSC section) is a key factor for this typical thermal properties. It is observed that the thermal stability of PNG system is higher than the PN system which can be attributed to the incorporation of rGO in blend matrix. In contrast, when rGO was added separately to PC and nylon phases, the thermal stability further increased which is higher for NGP as compared to PGN system. This increase in stability of the NGP system can be attributed to the selective dispersion of rGO in nylon phase, as discussed in the above sections. Nylon phase, which is the matrix phase contributes more towards the thermal stability of the system. Localization of rGO in this phase could have been delayed the degradation of polymer chains due to restricted thermal vibrations of polyamide chains adsorbed on rGO sheets. On other hand, in case of PGN system, the rGO sheets might localized in PC phase, which is the minor phase due to which the thermal stability of the matrix phase remained unaffected. However, the sole reinforcement in thermal stability can be attributed to better interfacial interaction between the nylon and PC phases where rGO sheets can act as a bridging agent between the PC and nylon phase as shown in Fig. 5.

4.5 Scratch hardness and depth indentation analysis

4.5.1 Scratch hardness (HS). Hardness is an ability of a material to resist penetration by other materials under the applied force.[54,55] Scratch analysis is a fundamental parameter to obtain material's hardness and nowadays it has often been used to measure hardness of polymeric materials. This analysis is simply based on harder material can easily scratch other material under a constant applied force, but not contrarily.[55] To measure micro-scratch hardness of prepared samples we have used flattened and dust free strip of specimens. Proper polishing (for smooth and dust free surface) is very necessary because a very minute disturbance on the surface might cause noticeable disorder in both force and depth measurement based on following fundamental equation.[55]

$$\mathrm{HS} = \frac{F_\mathrm{T}}{W \times D} \tag{1}$$

$$\mathrm{HS} = 2C\frac{\cos\varphi(1-\sin^2\theta)}{1-\sin\theta\cos\varphi\sqrt{1+(\tan\varphi\sin\varphi)^2}-\sin\varphi\cos^2\theta} \tag{2}$$

where F_T is horizontal applied force, W is the width of scratch surface and D is the depth of scratch surface, φ is the angle of internal friction, θ is back-rake angle, C is cohesion; an important part of unconfined compressive strength (UCS) of material and all these parameters of eqn (1) and (2) further depends on friction coefficient ($\mu = F_\mathrm{T}/F_\mathrm{V} = \tan\varphi$) which basic principle behind of scratch hardness testing.[55,56] In the present study, NGP shows maximum scratch resistance under the applied progressive scratch load. The tangential force curves of NGP showed very little fluctuations from the beginning to end of the testing range. Such little fluctuations for NGP is due to the prominent inertial effects and compact crystalline arrangement which strongly opposed progressive force applied by the indenter tip on the surface of NGP and *vice versa* for the pure polymers because of its highly amorphous nature. This drastic increase surface hardness for NGP is due the homogeneous distribution of rGO nanosheets as explained in DSC/TGA section.

The scratch hardness profile of neat blend is quite different from PNCs, it showed a zigzag curves corresponding applied progressive scratch load. Therefore, it is clear from the curve that pure blend cannot resist more applied progressive scratch load which is in good agreement with our TGA/DSC result. The slight increase of scratch hardness with very high fluctuations in tangential force for the neat blend as compared to the composites is probably due to the high percentage of nylon 66 and phase separation. The scratch hardness of PNG and PGN is nearly 40–45% less than the NGP however, higher than the pure polymers and neat blend. It can be attributed to the hindered motion of the polymeric chain owing to the bridging and the nucleation effect of the rGO nanosheets.

4.5.2 Depth indentation. The indentation technique which is usually used to investigate the mechanical properties of materials can also be utilized to measure residual stresses by controlling the indentation load indentation depth.[55,56] In order to determine the hardness of prepared PNCs in term of depth indentation, we have used depth sensing nano indentation technique.[55] The indentation response allows hardness and elastic modulus to be assessed. As the indenter is driven onto the surface of the material, an impression conforming to the shape of the indenter to some contact depth h_c appears.[56,57] Parameter contact depth (h_c) is an important parameter and it may be defined by the eqn (3)

$$h_\mathrm{c} = h - \varepsilon P/S \tag{3}$$

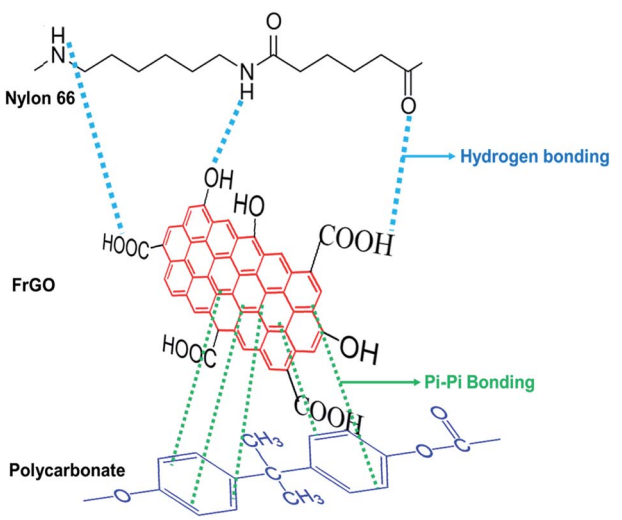

Fig. 5 Schematic representation of pi–pi interaction hydrogen bonding in synthesized PNCs.

where h is resulting penetration during the analysis, P is the load applied to the surface of the sample, ε is equal to 0.75 for Berkovich type indenter (as diamond tip; Young's modulus E = 1140 GPa, Poisson's ratio ν = 0.07 shown in Fig. 6) and S is unloading stiffness of sample.[57] In the present study, indentation load–displacement curve obtained at the stressed position was compared with that of measured in the non-stressed position, and then residual stress variations in the stressed position were calculated.[53–56] The analyzed indentation load–displacement curves are shown in Fig. 7 with different indentation depths for pure polymers and composites.

The load–depth indentation curve of studied polymeric materials revealed that (Fig. 7) magnitude of indentation depth corresponding to the volume of sample deformed due to the applied indentation force. From the graph, it is clear that nanocomposite NGP can bear the higher amount of applied force and therefore it can be used as high performance materials. On other hand PNG, PGN, PN, and pure polymers showing the trend as discussed in the TGA and FESEM sections.[56,57] In the case, of PNG, PGN, PN and pure polymers the residual post-scratch depths were measured during the analysis and it has be observed that majority of the scratches on the NGP have not significant residual post-scratch depths. This also supports that NGP possesses superior mechanical properties than the other tested specimen.

4.6 Rheology

To further explore dispersion of rGO in PC and nylon phases rheological analysis was carried out. Dispersion of nanofiller in polymer blend mainly affected by the kinetic and thermodynamic parameters. The viscosity against the shear rate is plotted in Fig. 8. The viscosity of pure polymers and all blend nanocomposites decreased exponentially with increased shear rate. It means all the polymeric systems displayed shear thinning phenomenon which may be due to the decrease in entanglement density of polymer chains under the influence of applied shear stress. Neat blend showed the notable decrease in viscosity as compared to pure polymers. Such notable decrease in the viscosity of pure blend can be ascribed to lower viscosity

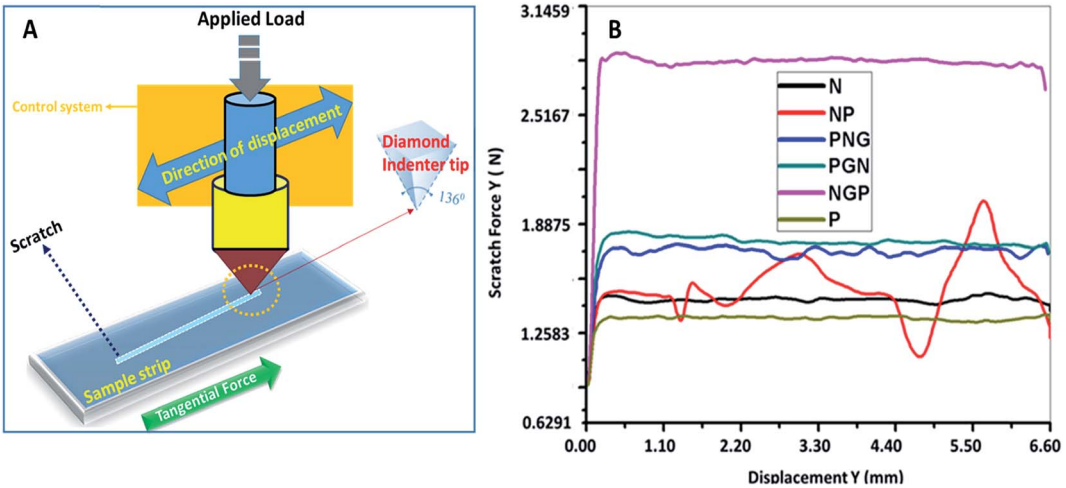

Fig. 6 (A) Schematic diagram showing scratch hardness and depth indentation testing and (B) depth profile results of a typical scratch on surface on the strip surface of pure polymers and prepared composites.

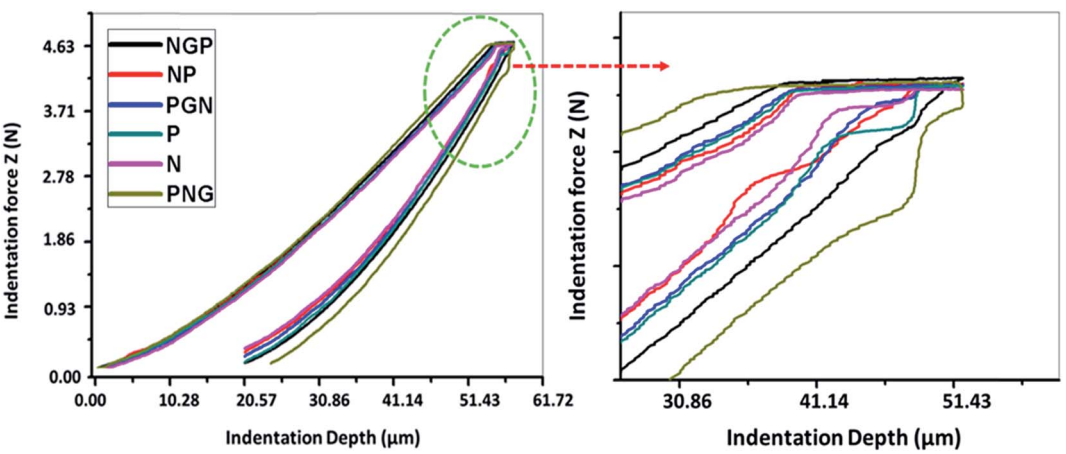

Fig. 7 The load–depth curves obtained from depth indentation experiment of the pure polymers and PNCs.

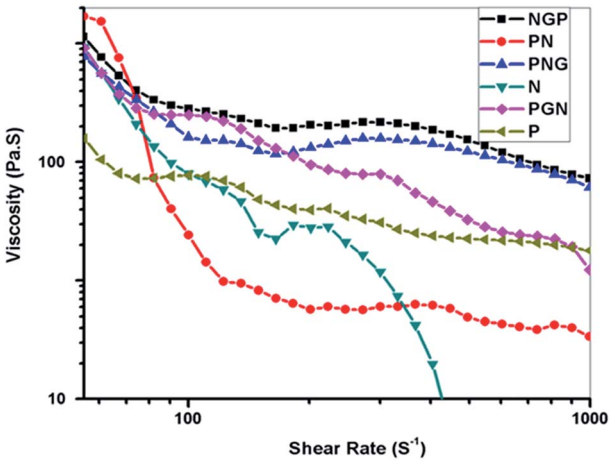

Fig. 8 Rheological behavior of polymer composites along with pure polymer and blends.

of nylon 66 as well as interfacial slippage between the blend components.[60,61] Among PC and nylon, at a lower shear rate the viscosity of nylon was found to be higher than PC. However, with the increase in shear rate the viscosity of nylon decreases drastically and lowered as compared to nylon. The viscosity behavior of rGO added systems (*i.e.* PNCs) increased as compared to the neat blend and pure polymers. This increase in viscosity is due to the incorporation of rGO, which restricted the interlayer slippage and movement of polymer chains and resultant increase in viscosity.[62] Highest viscosity was observed for NGP nanocomposite which can be ascribed to the homogeneous dispersion of rGO in both phases of nanocomposite. The viscosity of PNG system closely follows NGP blend system, but the viscosity was found to be lower as compared to NGP. This may be due to the viscosity effect where the viscosity of nylon is lower than the PC and during the fabrication of PNG system. In this case rGO sheets migrated to the nylon phase and dispersed properly under the high shear force owing to the interaction between polyamide chains and its functional groups. In addition, some of the rGO sheets might also disperse or migrate to the PC phase during mixing due to the interaction between PC and rGO which reduced the viscosity of PNG system. However, when rGO was first mixed with nylon and then with PC phase, the rGO nanosheets remained in nylon phase and induced higher viscosity of the system. In contrast, when rGO was first mixed with PC phase and then with nylon, the interaction between PC and rGO restricted the migration of rGO toward low viscous nylon phase and most of the rGO remained in minor PC phase, this why viscosity of PGN system found to be lower than NGP system. These results are in line with FTIR, XRD and DSC analysis.

4.7 FESEM analysis

Micrographic aspects of the composites have been studied to comprehend the change in the microstructure of the polymers owing to the incorporation of nanofiller in different mixing sequence. Fig. 9(a) represents FESEM images of the fractured surface of blend nanocomposites.[58,59] Neat blend showed droplet morphology where the PC phase is dispersed in nylon phase. Some fiber-like morphology can also be observed onto the fractured surface of the neat blend which may attribute to melt compounding under high shear pressure. For the neat blend, it can be seen that droplets are loosely held with nylon matrix which is an indication of a weak interaction at the interface between the same. The PNG system containing rGO shows similar droplet morphology due to the aggregation of rGO mainly in the PC phase and this can be observed in the high magnification FESEM image of PNG (inset). But the little increase in miscibility between the blend components for PNG can also be observed due to the nanosizing effect of rGO. It has believed that during the melt compounding rGO nanosheets first migrated to the nylon phase due to the lower viscosity of nylon 66 however, interaction with PC phase retarded this migration to nylon phase and so significant amount of the nanosheets trapped at the interface and prevented the easy pull out of PC phase (shown in the inset of PNG) from nylon 66. When rGO was first added to PC phase and then with nylon, rGO sheets were remained in PC phase due to strong interactions among PC and rGO and higher viscosity of PC phase which decreased the migration tendency of rGO (shown in the inset of PGN). In the case of PGN, a weak interfacial adhesion at the interface is very clear, which may be attributed to localization of rGO in highly viscous PC phase and result phase separation. The incorporation of rGO first in nylon phase and then its compounding with PC phase show better interfacial adhesion which may be due to the uniform dispersion of rGO in both nylon and PC (shown in the inset of NGP) phases. Fiber like morphology (inset) can be observed for the NGP system which is arises due to better interfacial compatibility at the interface of the blend. In summary, we can say that due to viscosity lag between nylon and PC; neat blend undergoes phase separation. But the incorporation of rGO in nylon phase enhanced its viscosity and during blending with PC phase, they have viscosity matching which resulted in better compatibility and hence droplet deformed as fibers. However, the same situation is not possible for the PNG and PGN and result in partial miscibility. A schematic representation for the dispersion rGO and morphology is showed in Fig. 9(b).

4.8 Mechanical testing

Fig. 10a–c represent the tensile strength, young modulus and elongation at break of the pure polymer, blend and nanocomposites. The value of tensile strength, young modulus, and elongation at break for pure polymers is closely similar to the earlier reports.[22,23,56] In the case of a pure blend, these three mechanical parameters decreased emphatically as compared to pure nylon 66 and polycarbonate which reveals a very poor adhesion and a high degree of phase separation between the same. Both PNG and PGN nanocomposites possessed higher tensile strength, young modulus and elongation than pure polymers and neat blend this is due to the bridging effect of rGO on polymer matrices.[61,62] This recommends an enhancement in interfacial adhesion between polymer matrices which facilitate proper stress transfer on each component of nanocomposites.

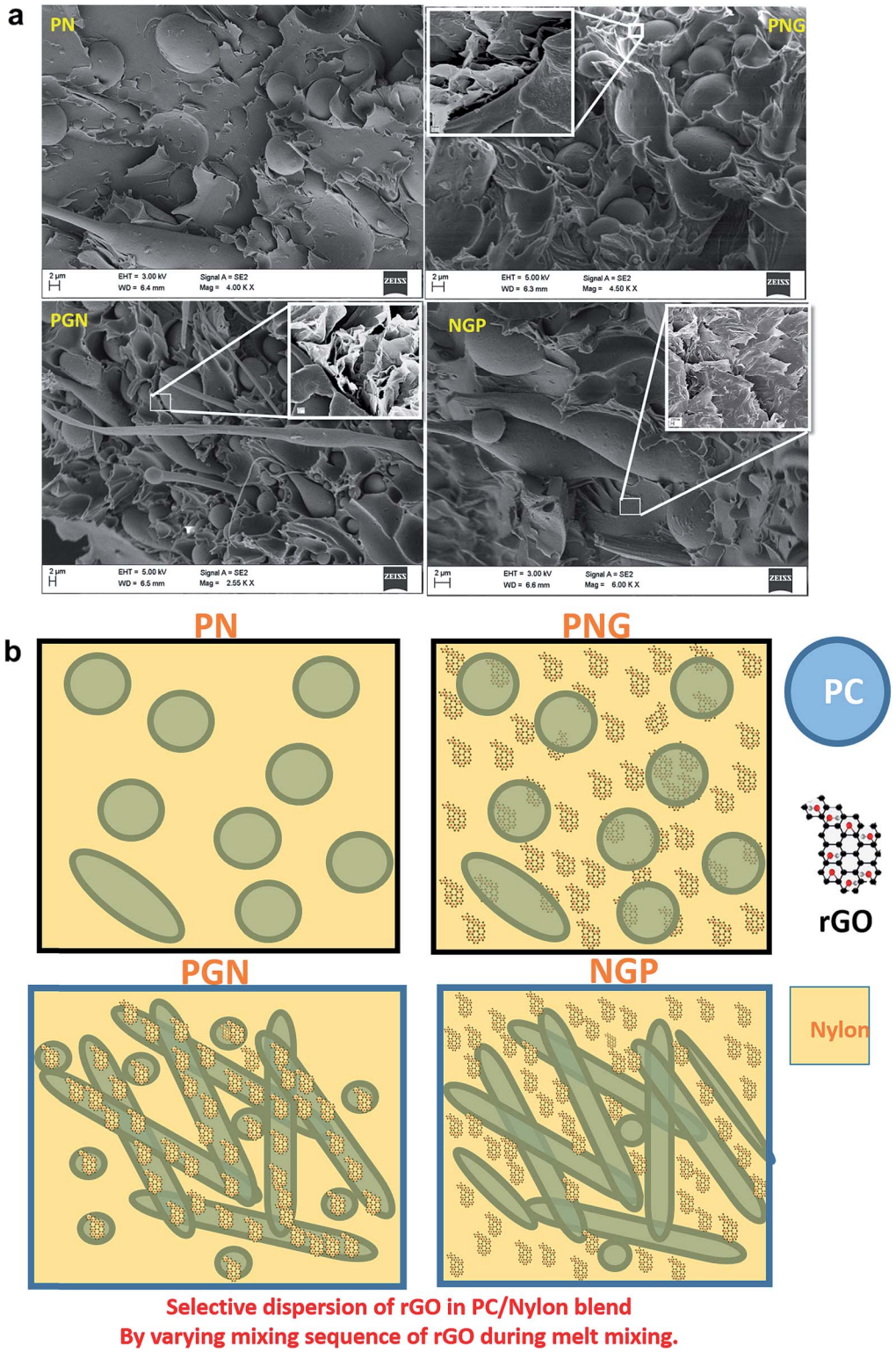

Fig. 9 (a) FESEM micrograph of PN, PNG, PGN and NGP at low magnification and inset shows the magnified image of marked sections. (b) Schematic representation of selective dispersion of rGO in blend matrix.

Thus, bridging effect improved both the strength and modulus at interfaces of nanocomposites that need more energy to pull out the nylon 66 phase from PC and result resists the fracture and increased the tensile strength.[61] Interestingly, the mechanical strength of PGN is lower than PNG which can be attributed to the weaker adhesion at the interfaces of the same which ultimately depends on mixing sequence of rGO as mentioned in the previous sections.[61,62] This result was further

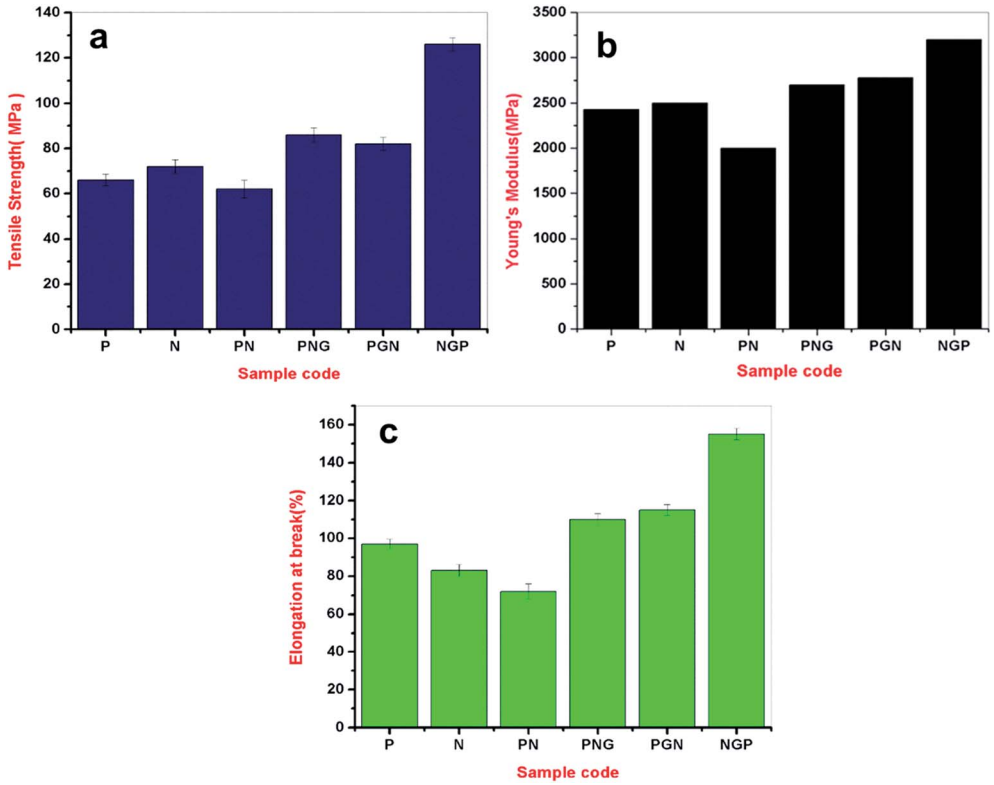

Fig. 10 Tensile modulus, Young modulus and elongation at break of the prepared nanocomposites along with pure polymers.

supplemented by the swelling study where NGP shows the least uptake of different solvents as compared to other composites and therefore better stability in the case of NGP (ESI† file).

In summary, we can say that melt viscosity of nylon 66/polycarbonates and mixing sequence of rGO played an important role to define miscibility and physical properties of studied blend systems. Nanocomposite NGP showed outstanding thermo-mechanical properties due to the homogeneous dispersion of rGO into the matrices of nanocomposites. Such dispersion of rGO attributed to the migration of excess rGO from nylon 66 to PC phase when rGO first mixed with nylon 66. However, when rGO first dispersed in polycarbonate and then with nylon; so, due to the strong hydrogen bonding and π–π interaction of rGO with PC, then their further migration into nylon 66 is not possible and therefore aggregation of rGO in a single blend partner. In the case of PNG, thermo-mechanical properties found superior to PGN and inferior in comparison to NGP and it may ascribe to partial distribution of rGO in polymer matrices of blend system.

5. Conclusion

Nylon 66/polycarbonate based blend nanocomposites was reinforced using few layered reduced graphene oxide (rGO) nanofiller. The incorporation of this nanofiller to nylon 66/polycarbonate provided an amazing increase in thermo-mechanical properties of composites attributed to the bridging and the nucleation effect of rGO nanosheets. The XRD investigation revealed that crystal growth is less prominent in the case of composite NGP owing to the homogeneous distribution of rGO in the both polymer matrices. However, crystal growth in the case other composites are intense due to the aggregation of rGO in selectively in polycarbonate phase. FTIR analysis showing similar result and gives a strong support for the existence of nonbonding interactions between polycarbonate, nylon 66 and rGO. FESEM analysis of a fractured surface revealed better interfacial adhesion for the NGP system due to the homogeneous dispersion of rGO and result in superior mechanical strength in the case of NGP than other fabricated blend systems. These investigations proved that mixing sequence of rGO in nylon 66/polycarbonate blend system can influence the thermal and mechanical properties of blend nanocomposites. Furthermore, thermal stability and chemical inertness for all the blend nanocomposites was boosted due to the addition of rGO in comparison to neat blend.

Acknowledgements

We acknowledge DST (SERB), INDIA for their financial support for this work *via* sanction number-SERB/F/4910/2013-14. Authors are very grateful to Prof. Ashis Mallick, Dept. of Mechanical Engineering, IIT(ISM), Dhanbad for the kind permission related to micro-hardness and scratch testing.

References

1 L. A. Utracki, *Commercial Polymer Blends*, Springer, US, 1998. DOI: 10.1007/978-1-4615-5789-0.

2 V. K. Thakur, M. K. Thakur, P. Raghavan and M. R. Kessler, *ACS Sustainable Chem. Eng.*, 2014, **5**, 1072.
3 M. T. Albdiry, B. F. Yousif, H. Ku and K. T. Lau, *J. Compos. Mater.*, 2013, **9**, 1093.
4 W. K. Chee, H. N. Lim, N. M. Huang and I. Harrison, *RSC Adv.*, 2015, **83**, 68014.
5 R. K. Layek and A. K. Nandi, *Polymer*, 2013, **19**, 5087.
6 A. S. F. Santos, J. A. M. Agnelli, D. W. Trevisan and S. Manrich, *Polym. Degrad. Stab.*, 2002, **3**, 441.
7 I. C. Sanchez and R. H. Lacombe, *Macromolecules*, 1978, **6**, 1145.
8 A. V. G. Ruzette and A. M. Mayes, *Macromolecules*, 2001, **6**, 1894.
9 T. Hirata, H. Matsuno, M. Tanaka and K. Tanaka, *Phys. Chem. Chem. Phys.*, 2011, **11**, 4928.
10 Y. Zare, *Waste Manag.*, 2013, **3**, 598.
11 L. T. Yan and X. M. Xie, *Prog. Polym. Sci.*, 2013, **2**, 369.
12 M. Xanthos and S. S. Dagli, *Polym. Eng. Sci.*, 1991, **13**, 929.
13 E. A. Eastwood and M. D. Dadmun, *Macromolecules*, 2002, **13**, 5069.
14 F. Gubbels, R. Jérôme, E. Vanlathem, R. Deltour, S. Blacher and F. Brouers, *Chem. Mater.*, 1998, **5**, 1227.
15 R. Sengupta, M. Bhattacharya, S. Bandyopadhyay and A. K. Bhowmick, *Prog. Polym. Sci.*, 2011, **5**, 638.
16 J. Bijwe, *Polym. Compos.*, 1997, **3**, 378.
17 H. Ishida and J. L. Koenig, *Polym. Eng. Sci.*, 1978, **2**, 128.
18 S. Satapathy, A. Nag and G. B. Nando, *Process Saf. Environ. Prot.*, 2010, **2**, 131.
19 P. Bordes, E. Pollet and L. Avérous, *Prog. Polym. Sci.*, 2009, **2**, 125.
20 I. A. Rahman and V. Padavettan, *J. Nanomater.*, 2012, **2014**, 132424.
21 J. N. Coleman, U. Khan, W. J. Blau and Y. K. Gun'ko, *Carbon*, 2006, **9**, 1624.
22 X. L. Xie, Y. W. Mai and X. P. Zhou, *Mater. Sci. Eng., R*, 2005, **4**, 89.
23 A. L. Martínez-Hernández, V. M. Castaño, J. L. Rivera-Armenta, F. J. Medellín-Rodríguez and G. Martínez-Barrera, *J. Nanomater.*, 2014, **2014**, 670261.
24 G. Mittal, V. Dhand, K. Y. Rhee, S. J. Park and W. R. Lee, *J. Ind. Eng. Chem.*, 2015, **21**, 11.
25 S. M. Thomas, R. DiCosimo and V. Nagarajan, *Trends Biotechnol.*, 2002, **6**, 238.
26 M. Moniruzzaman, J. Chattopadhyay, W. E. Billups and K. I. Winey, *Nano Lett.*, 2007, **5**, 1178.
27 A. Larsson and H. Dérand, *J. Colloid Interface Sci.*, 2002, **1**, 214.
28 S. K. Tiwari, V. Kumar, A. Huczko, R. Oraon, A. De Adhikari and G. C. Nayak, *Crit. Rev. Solid State Mater. Sci.*, 2016, **4**, 257.
29 S. K. Tiwari, R. Oraon, A. De Adhikari and G. C. Nayak, *J. Appl. Polym. Sci.*, 2017, 45062, DOI: 10.1002/app.45062.
30 W. Choi, I. Lahiri, R. Seelaboyina and Y. S. Kang, *Crit. Rev. Solid State Mater. Sci.*, 2010, **1**, 52.
31 Y. Cao, J. Feng and P. Wu, *J. Mater. Chem.*, 2012, **30**, 14997.
32 C. Bao, L. Song, W. Xing, B. Yuan, C. A. Wilkie, J. Huang, Y. Guo and Y. Hu, *J. Mater. Chem.*, 2012, **13**, 6088.
33 M. Cano, U. Khan, T. Sainsbury, A. O'Neill, Z. Wang, I. T. McGovern, W. K. Maser, A. M. Benito and J. N. Coleman, *Carbon*, 2013, **52**, 363.
34 P. Verma, P. Saini, R. S. Malik and V. Choudhary, *Carbon*, 2015, **89**, 308.
35 A. M. Pinto, J. Martins, J. A. Moreira, A. M. Mendes and F. D. Magalhães, *Polym. Int.*, 2013, **6**, 928.
36 D. C. Marcano, D. V. Kosynkin, J. M. Berlin, A. Sinitskii, Z. Sun, A. Slesarev, L. B. Alemany, W. Lu and J. M. Tour, *ACS Nano*, 2010, **8**, 4806.
37 S. K. Tiwari, A. Huczko, R. Oraon, A. De Adhikari and G. C. Nayak, *J. Mater. Sci.*, 2016, **13**, 6156.
38 D. I. Christensen, U.S. Patent, 3,597,498, Monsanto Co, 1971.
39 http://hdl.handle.net/2292/319.
40 C. Bao, L. Song, W. Xing, B. Yuan, C. A. Wilkie, J. Huang, Y. Guo and Y. Hu, *J. Mater. Chem.*, 2012, **13**, 6088.
41 E. Ghorbel, I. Hadriche, G. Casalino and N. Masmoudi, *Materials*, 2014, **1**, 375.
42 J. Charles, G. R. Ramkumaar, S. Azhagiri and S. Gunasekaran, *E-J. Chem.*, 2009, **1**, 23.
43 B. R. Guduri and A. S. Luyt, *J. Nanosci. Nanotechnol.*, 2008, **4**, 1880.
44 J. H. Dumbleton, D. R. Buchanan and B. B. Bowles, *J. Appl. Polym. Sci.*, 1968, **9**, 2067.
45 H. W. Ha, A. Choudhury, T. Kamal, D. H. Kim and S. Y. Park, *ACS Appl. Mater. Interfaces*, 2012, **9**, 4623.
46 D. Parviz, S. Das, H. T. Ahmed, F. Irin, S. Bhattacharia and M. J. Green, *ACS Nano*, 2012, **10**, 8857.
47 G. Hatui, A. Malas, P. Bhattacharya, S. Dhibar, M. K. Kundu and C. K. Das, *J. Alloys Compd.*, 2015, **619**, 709.
48 I. M. Kalogeras and W. Brostow, *J. Polym. Sci., Part B: Polym. Phys.*, 2009, **1**, 80.
49 W. Brostow, R. Chiu, I. M. Kalogeras and A. Vassilikou-Dova, *Mater. Lett.*, 2008, **17**, 3152.
50 Y. He, B. Zhu and Y. Inoue, *Prog. Polym. Sci.*, 2004, **10**, 1021.
51 T. Park and S. C. Zimmerman, *J. Am. Chem. Soc.*, 2006, **35**, 11582.
52 B. A. Sweileh, Y. M. Al-Hiari, M. H. Kailani and H. A. Mohammad, *Molecules*, 2010, **5**, 3661.
53 A. J. Crosby and J. Y. Lee, *Polym. Rev.*, 2007, **2**, 217.
54 D. W. Seong, J. S. Yeo and S. H. Hwang, *J. Ind. Eng. Chem.*, 2016, **36**, 251.
55 http://ksm.fsv.cvut.cz/~nemecek/teaching/dmpo/clanky/2015/Kadlicek_zav%20prace_Scratch%20test.pdf, accessed 2016.
56 J. L. Bucaille, E. Felder and G. Hochstetter, *Wear*, 2001, **5**, 422.
57 K. Friedrich, H. J. Sue, P. Liu and A. A. Almajid, *Tribol. Int.*, 2011, **9**, 1032.
58 M. Mukherjee, T. Das, R. Rajasekar, S. Bose, S. Kumar and C. K. Das, *Composites, Part A*, 2009, **8**, 1291.
59 R. Mahendran, D. Sridharan, K. Santhakumar, T. A. Selvakumar, P. Rajasekar and J. H. Jang, *Indian J. Eng. Mater. Sci.*, 2016, **2016**, 4169409.
60 H. Kim and C. W. Macosko, *Polymer*, 2009, **15**, 3797.
61 J. Zhou, I. A. Ventura and G. Lubineau, *Ind. Eng. Chem. Res.*, 2014, **9**, 3539.
62 J. Zhou and G. Lubineau, *ACS Appl. Mater. Interfaces*, 2013, **13**, 6189.